



**HAL**  
open science

## Porous Silicon Preparation by Electrochemical Etching in Ionic Liquids

Evgeniya A. Saverina, Daria Y. Zinchenko, Sofia D. Farafonova, Alexey S. Galushko, Andrei Novikov, Maxim Gorbachevskii, Valentine P. Ananikov, Mikhail P. Egorov, Viatcheslav Jouikov, Mikhail A. Syroeshkin

► **To cite this version:**

Evgeniya A. Saverina, Daria Y. Zinchenko, Sofia D. Farafonova, Alexey S. Galushko, Andrei Novikov, et al.. Porous Silicon Preparation by Electrochemical Etching in Ionic Liquids. ACS Sustainable Chemistry & Engineering, 2020, 8 (27), pp.10259-10264. 10.1021/acssuschemeng.0c03133. hal-02928603

**HAL Id: hal-02928603**

**<https://hal.science/hal-02928603>**

Submitted on 10 Sep 2020

**HAL** is a multi-disciplinary open access archive for the deposit and dissemination of scientific research documents, whether they are published or not. The documents may come from teaching and research institutions in France or abroad, or from public or private research centers.

L'archive ouverte pluridisciplinaire **HAL**, est destinée au dépôt et à la diffusion de documents scientifiques de niveau recherche, publiés ou non, émanant des établissements d'enseignement et de recherche français ou étrangers, des laboratoires publics ou privés.

# Porous silicon preparation by electrochemical etching in ionic liquids

*Evgeniya A. Saverina,<sup>1,2</sup> Daria Yu. Zinchenko,<sup>1</sup> Sofia D. Farafonova,<sup>1,3</sup> Alexey S.*

*Galushko,<sup>1</sup>*

*Andrei A. Novikov,<sup>4</sup> Maxim V. Gorbachevskii,<sup>4</sup> Valentine P. Ananikov,<sup>1</sup> Mikhail P.*

*Egorov,<sup>1</sup>*

*Viatcheslav V. Jouikov,<sup>\*2</sup> Mikhail A. Syroeshkin<sup>\*1</sup>*

<sup>1</sup>N. D. Zelinsky Institute of Organic Chemistry, Moscow, Russia

<sup>2</sup>University of Rennes, UMR CNRS 6226, ISCR (Institut des Sciences Chimiques de Rennes), Rennes, France

<sup>3</sup>Dmitry Mendeleev University of Chemical Technology of Russia, Moscow, Russia

<sup>4</sup>Gubkin University, Moscow, 119991, Russia

1  
2  
3 **Keywords:** porous silicon, electrochemical etching, HF-free, fluorescence, confocal  
4  
5  
6  
7 microscopy, green chemistry.  
8  
9

10  
11  
12  
13  
14  
15 **Abstract:** Anodic etching of n-type {111} silicon in ionic liquid (IL) systems ([RMIM][X], R  
16 = H, Bu; X = BF<sub>4</sub><sup>-</sup>, PF<sub>6</sub><sup>-</sup>), realized under galvanostatic conditions and room temperature,  
17  
18 allowed the formation of porous silicon surfaces with different pore morphology  
19  
20 depending on the etching time, current density and the IL used. The study of the effect  
21  
22 of water content in IL on the etching process has shown water content of 1% to be  
23  
24 optimal. The role of the anion on the etching process was elucidated using 1-  
25  
26 methylimidazolium tetrafluoroborate ([HMIM][BF<sub>4</sub>]) and 1-methylimidazolium  
27  
28 hexafluorophosphate ([HMIM][PF<sub>6</sub>]) IL systems. [HMIM][BF<sub>4</sub>] was found to be most  
29  
30 efficient for the formation of silicon nanostructured array with a pore size of 30-80 nm.  
31  
32  
33 The thus prepared porous silicon samples show fluorescence in blue light (475 nm).  
34  
35  
36  
37  
38  
39  
40  
41  
42  
43  
44  
45  
46  
47  
48  
49  
50  
51  
52  
53  
54  
55  
56  
57  
58  
59  
60  
The NMR spectra of [HMIM][BF<sub>4</sub>] ionic liquid before and after etching does not show

1  
2  
3 noticeable changes, which makes possible to consider this IL as a potentially recyclable  
4  
5  
6  
7 etching agent.  
8  
9  
10  
11  
12  
13  
14  
15

## 16 Introduction

17  
18  
19  
20

21 Silicon-based materials, in particular porous silicon (PSi), are of high demand in the  
22  
23 materials science. Besides dominating solar cells market<sup>[1-4]</sup> silicon and its porous form  
24  
25 are widely used in various research fields such as optoelectronics,<sup>[5-6]</sup> biosensing<sup>[7-9]</sup> and  
26  
27  
28 biomedical applications.<sup>[10-16]</sup>  
29  
30  
31  
32  
33  
34  
35

36 The primary method of obtaining PSi is oxidative etching of a non-porous silicon  
37  
38 precursor in hydrofluoric acid solutions.<sup>[17]</sup> In electrochemical version of silicon etching  
39  
40 in fluoride solutions the process can be carried out both in potentiostatic and in  
41  
42  
43 galvanostatic mode; the latter option is often preferable because of easier control of the  
44  
45  
46  
47  
48  
49 process.<sup>[9]</sup>  
50  
51  
52  
53  
54  
55  
56  
57  
58  
59  
60

1  
2  
3  
4 Although the extreme safety hazards of hydrofluoric acid for nature and humans are  
5  
6  
7 well known,<sup>[18]</sup> using HF in PSi production seems unavoidable since it is needed for  
8  
9  
10 removal of native oxides on silicon surface and for binding silicon in etching products.  
11  
12

13  
14 The search for different approaches for replacing HF acid by more environmental-  
15  
16  
17 friendly agents is of great interest in the field of silicon etching<sup>[19,20]</sup> and in other areas of  
18  
19  
20 materials science.<sup>[21-23]</sup>  
21  
22

23  
24  
25 A method of silicon etching replacing HF with silicophilic reagents, in particular, salts of  
26  
27  
28 pyridine or N-aromatic bases with tetrafluoroboric acid in an organic solvent was  
29  
30  
31 previously proposed.<sup>[19]</sup> It should be noted that for etching silicon in such systems, it is  
32  
33  
34 necessary to use the salts solutions of high concentration. In this regard, etching  
35  
36  
37 systems based on protic ionic liquids,<sup>[24]</sup> combining solvent and supporting salt in one  
38  
39  
40 compound<sup>[25-26]</sup> that were successfully used in surface electro-chemistry<sup>[27]</sup> might be  
41  
42  
43 more promising.  
44  
45  
46  
47  
48  
49  
50  
51  
52  
53  
54  
55  
56  
57  
58  
59  
60

Besides entirely merited attention and wide use in almost all chemistry-related areas,<sup>[28-</sup>

<sup>31]</sup> ionic liquids permit to address and in many cases to improve very important ecological issues.

In this work, we propose a simple, environment-friendly, and efficient technique for preparing porous silicon by means of an HF-free electrochemical etching in the ionic liquid medium (primarily derivatives of 1-methylimidazolium, [HMIM][BF<sub>4</sub>]). This method allows one to prepare a uniformly porous silicon surface with the possibility of controlling the pore size.

## Results and discussion

The [HMIM][BF<sub>4</sub>] ionic liquid was synthesized by stirring 1-methylimidazole with tetrafluoroboric acid in appr. 1:1 molar ratio with minimal excess of 1-methylimidazole to prevent the presence of HBF<sub>4</sub> in product. After that, the resulting solution was evaporated, washed with ethyl acetate and dried under vacuum according to <sup>[32]</sup>.

Several samples of [HMIM][BF<sub>4</sub>] were then prepared with a water content of 1%, 5%, and 10%, controlled by Fischer titration.<sup>[33]</sup> Synthesized in the similar way [HMIM][PF<sub>6</sub>]

1  
2  
3  
4 was conditioned to water content of 2%. In contrast to dry ILs, such wet ionic liquids (w-  
5  
6  
7 IL) remain liquid at room temperature; this enables using them for silicon etching under  
8  
9  
10 the ambient conditions without heating which is otherwise needed to liquefy these ILs.  
11  
12

13  
14  
15 These w-IL were then tested for etching silicon and revealing the influence of current  
16  
17  
18 density and etching time on the morphology of the obtained samples.  
19  
20

21  
22  
23 A polished n-type (111) oriented single-crystal silicon wafer was used (Fig. S1) for this  
24  
25  
26 purpose. The etching was carried out at room temperature in a galvanostatic mode,  
27  
28  
29 using a specially designed polytetrafluorethylene (PTFE) cell (Fig. 1). The cell was fitted  
30  
31  
32 with a PTFE nut with a 4 mm hole protecting the Si sample so that the etching area,  
33  
34  
35 limited by the hole, remains constant throughout all experiments. A platinum grid was  
36  
37  
38 used as a cathode.  
39  
40  
41  
42  
43  
44  
45  
46  
47  
48  
49  
50  
51  
52  
53  
54  
55  
56  
57  
58  
59  
60

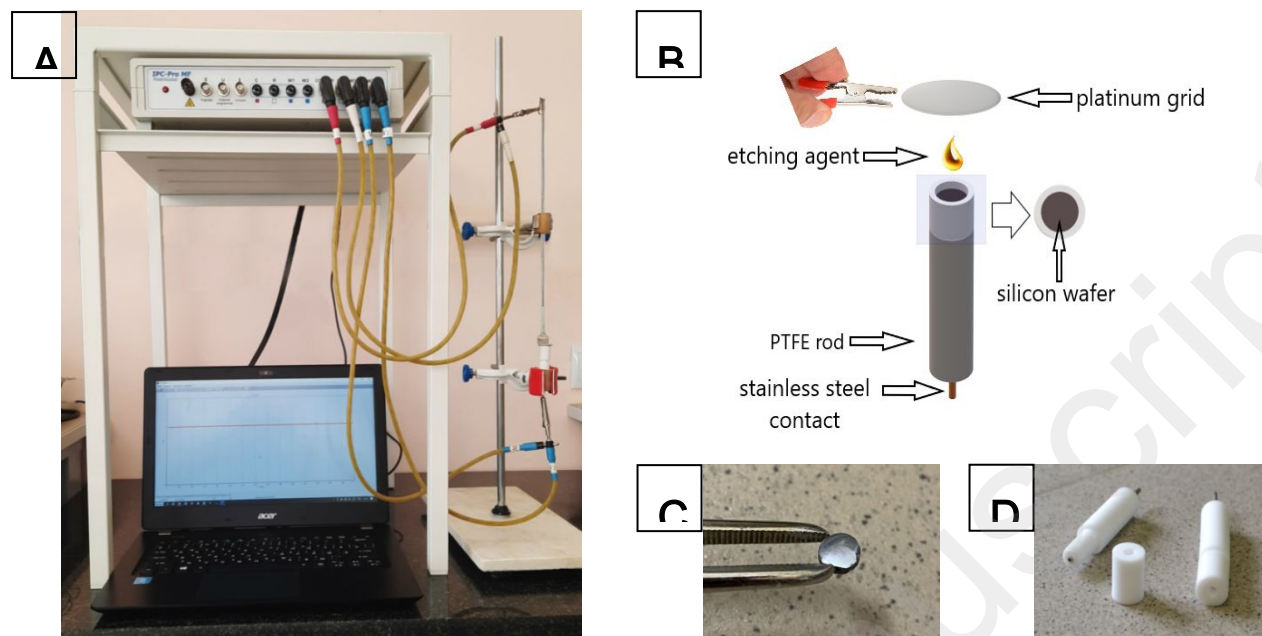


**Figure 1.** Photograph of a silicon etching setup (A), the scheme of assembling the etching PTFE cell (B), a polished silicon wafer used in the experiments (C), and a PTFE cell (D) for mounting the sample for etching.

We found that etching in 1% [HMIM][BF<sub>4</sub>] w-IL system at a current density  $j = 8 \text{ mA/cm}^2$  during 30 min results in the development of significant roughness of the surface of silicon wafer (Fig. 2 left). Further increase in etching time leads to the formation of a porous surface.

In particular, a uniform mesoporous surface with the irregularly shaped pores sized of  $31 \pm 2 \text{ nm}$  separated by  $8 \pm 1 \text{ nm}$  walls was obtained after a 5 hours etching (Fig. 2 right).

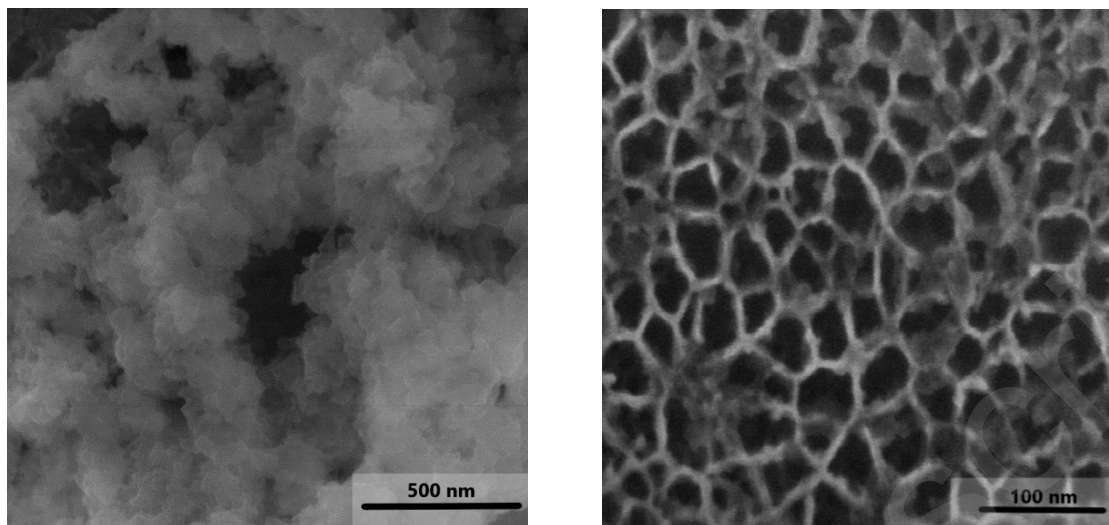
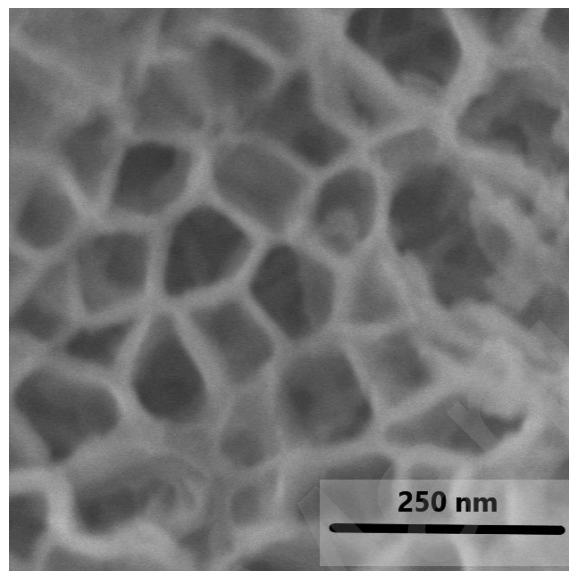


**Figure 2.** Scanning electron microscope (SEM) images of porous silicon obtained by etching in 1% [HMIM][BF<sub>4</sub>] w-IL system at a current density 8 mA/cm<sup>2</sup> during 30 minutes (left) and 5 hours (right).

When etching in HF-based systems, higher current densities are known to increase the pore size and depth.<sup>[34-35]</sup> This trend was also observed during the etching of silicon in [HMIM][BF<sub>4</sub>]-based w-IL system. Fig. 3 shows an scanning electron microscope (SEM) picture of the sample obtained by etching a silicon wafer at  $j = 24 \text{ mA/cm}^2$  for 1 hour.

It can be seen that the pores at thus prepared homogeneous porous surface are larger than those observed after etching for 5 hours at  $j = 8 \text{ mA/cm}^2$ . Now, the pore size and

1  
2  
3 the thickness of the separating walls are increased up to  $79\pm 6$  nm and  $21\pm 1$  nm,  
4  
5  
6  
7 respectively. It is noteworthy that the majority of the cells formed are 4 or 5-faceted.  
8  
9



32 **Figure 3.** SEM image of porous silicon obtained by etching in 1% [HMIM][BF<sub>4</sub>] w-IL  
33  
34  
35 system within 1 hour at a current density of 24 mA/cm<sup>2</sup>.  
36  
37

38  
39  
40 During etching gas formation is observed, but the change in the amount of water cannot  
41  
42  
43 be determined within the measurement accuracy, and after the process the system  
44  
45  
46 remains liquid. It contain white amorphous solid.  
47  
48

49  
50  
51 The increase of water content in the IL significantly affects the nature of etching. So, at  
52  
53  
54  
55 5% water in IL the morphology of the formed layer changed now resembling to a  
56  
57  
58  
59  
60

1  
2  
3 network of bulges around deeper etching zones of commensurate size (Fig. S2). This  
4  
5  
6  
7 case is intermediate between the cellular structure (Fig. 2, 3) and a spongy surface  
8  
9  
10 when etching is achieved with higher water content (10%) (Fig. S3).  
11  
12

13  
14  
15 Elucidating the role of anion in the etching process encounters the intrinsic difficulties of  
16  
17  
18 strongly varying electrochemical properties of ILs when changing the anion.  
19  
20

21  
22 Alkylimidazolium ILs with  $\text{PF}_6^-$  anion have about ten times higher viscosity and ten-fold  
23  
24  
25 lower conductivity than with  $\text{BF}_4^-$ ,<sup>[36]</sup> which dramatically alters etching efficiency with  
26  
27  
28  
29 [HMIM][ $\text{PF}_6$ ]. The process becomes non-uniform developing locally (Fig. S5, S6),  
30  
31  
32 though at the bottom of the affected zones the dilution of the IL with etching products  
33  
34  
35 makes the conditions closer to those with less viscous [HMIM][ $\text{BF}_4$ ] and leads to the  
36  
37  
38 formation of a similar cellular structure (Fig. S6). Thus, changing the counterion to  $\text{PF}_6^-$   
39  
40  
41  
42 has significant impact on the surface structure and the viscosity effects point at a  
43  
44  
45 diffusion-based process.  
46  
47  
48  
49

50  
51 When the difference in viscosity/conductivity is smaller, ca. 2 times, finer tuning of  
52  
53  
54 etching properties is seen. An isotropic electropolishing occurs (Fig. S4) with  
55  
56  
57  
58  
59  
60

1  
2  
3  
4 [BMIM][BF<sub>4</sub>] (108.25 cP<sup>[37]</sup> and 3.53 mS/cm<sup>[38]</sup>), whereas an intermediate regime was  
5  
6  
7 observed with [BMIM][PF<sub>6</sub>] (284.49 cP<sup>[37]</sup> and 1.65 mS/cm<sup>[39]</sup>) when mesoporous  
8  
9  
10 etching (Fig. 4 a) goes concomitantly with the formation of a sub 100 nm pattern (Fig. 4  
11  
12  
13  
14 c).

15  
16  
17  
18 It should be noted that the formation of pores occurs without significant oxidation of the  
19  
20  
21 silicon surface, as the fraction of silicon oxide in the resulting material is less than 1.5%  
22  
23  
24  
25 (according energy dispersive X-ray spectroscopy (EDS) data).  
26  
27

28  
29  
30 One of the essential qualities of porous silicon is its strong fluorescence.<sup>[40-41]</sup> The  
31  
32  
33 fluorescence spectrum of a porous silicon sample obtained by etching in 1%  
34  
35  
36 [HMIM][BF<sub>4</sub>] w-IL system at a current density of 8 mA/cm<sup>2</sup> for 6 hours (Fig. 5) has a  
37  
38  
39  
40 maximum in blue light at 475 nm. A more detailed study of the optical properties of the  
41  
42  
43  
44 material is the subject of further study.  
45  
46  
47  
48  
49  
50  
51  
52  
53  
54  
55  
56  
57  
58  
59  
60

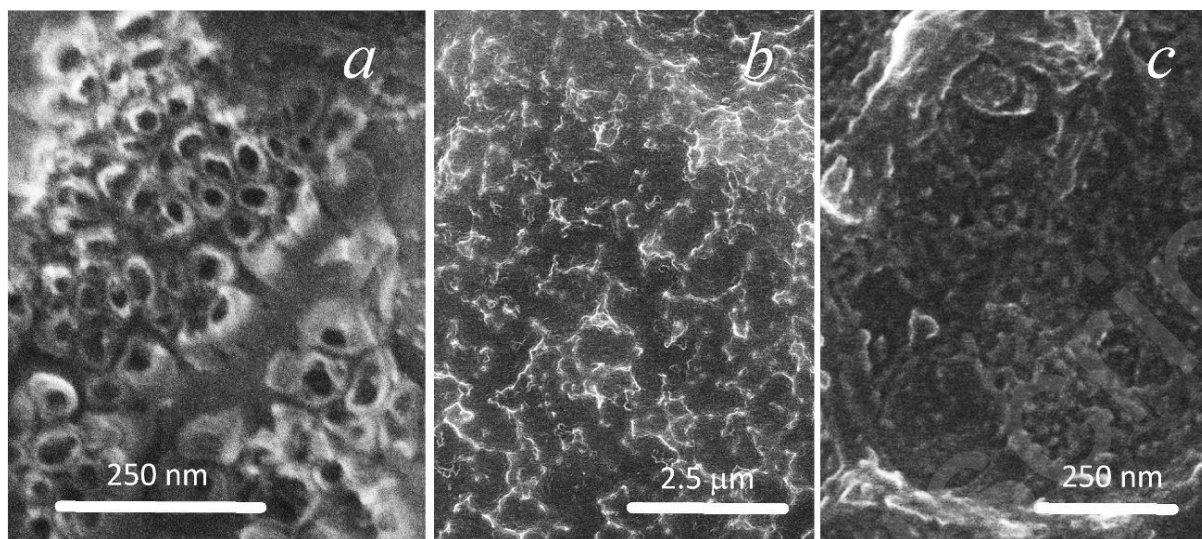
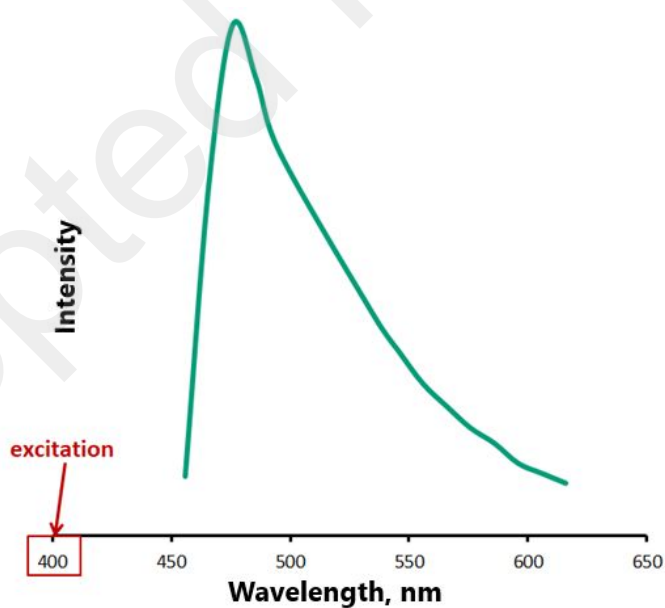


**Figure 4.** SEM images of a silicon samples etched in w-ILs with  $[PF_6^-]$  anion: (a)  $[HMIM][PF_6]$  (water content 2%) for 1 hour at  $j = 24 \text{ mA/cm}^2$ , (b) and (c)  $[BMIM][PF_6]$  (water content 1%) for 1 hour at  $j = 24 \text{ mA/cm}^2$ .



1  
2  
3  
4 **Figure 5.** The fluorescence spectrum (excitation at 401 nm) of a porous silicon sample  
5  
6  
7 obtained by etching in 1% [HMIM][BF<sub>4</sub>] w-IL system during 6 hours at  $j = 8 \text{ mA/cm}^2$ .  
8  
9

10  
11 Raman spectra of the studied samples (Fig. S19, S20) are quite similar, with the more  
12  
13 pronounced 2TO mode of the etched silicon, especially with the 532 nm excitation.  
14  
15  
16

17  
18  
19 The IL used for preparing the wafer as in Fig. 2 (right) was diluted with CD<sub>3</sub>CN, and a  
20  
21 comprehensive range of <sup>1</sup>H, <sup>13</sup>C, <sup>11</sup>B, and <sup>19</sup>F NMR spectra were recorded. Comparison  
22  
23 of NMR spectra of this IL before and after etching showed that it does not decompose  
24  
25 during the etching process (all signals at all nuclei before and after etching are  
26  
27 completely identical and only the acidic proton signal shifts to the region of the high  
28  
29 fields, which indicates a some decrease in pH <sup>[42]</sup>) and it can be considered as a  
30  
31 potentially recyclable etching agent (see Fig. S7-S14). Of course, the interpretation that  
32  
33 the ionic liquids will be recyclable because there is no degradation of the IL as  
34  
35 determined by NMR spectroscopy is just a preliminary investigation; and, we will need  
36  
37 to be examined more closely in the future including examination of the purity of the IL  
38  
39  
40  
41  
42  
43  
44  
45  
46  
47  
48  
49  
50  
51  
52  
53  
54  
55  
56  
57  
58  
59  
60 after several uses and using a more sensitive technique.

## Experimental

*Reagents, solvents, and materials.* [BMIM][BF<sub>4</sub>] (99 %), used for etching, was supplied by Sigma Aldrich. [BMIM][PF<sub>6</sub>] (99%) was supplied by ABCR. [HMIM][BF<sub>4</sub>] and [HMIM][PF<sub>6</sub>] were prepared from 1-methylimidazol, 99 % (Acros) and fluoroboric acid, 48 wt % (Acros) or hexafluorophosphoric acid, 55 wt % (Sigma Aldrich) respectively.

Ionic liquid systems were washed with ethyl acetate (Acros).

The n-type (111) single-crystalline silicon wafer (d = 5 mm, thickness = 2 mm) was polished to a high gloss with chromium oxide GOI polishing paste and then degreased with isopropyl alcohol (SEM/EDS - see Fig.S1).

*Synthesis of ionic liquids.* [HMIM][BF<sub>4</sub>] was synthesized according to known literary technic.<sup>[32]</sup> The synthesis of [HMIM][PF<sub>6</sub>] was carried out similarly.

The purity and structure of prepared [HMIM][BF<sub>4</sub>], [HMIM][PF<sub>6</sub>] were confirmed by <sup>1</sup>H, <sup>13</sup>C, <sup>11</sup>B, <sup>19</sup>F and <sup>31</sup>P NMR analysis (see SI). The NMR spectra of [HMIM][BF<sub>4</sub>] in CD<sub>3</sub>CN: <sup>1</sup>H NMR (600 MHz): 3.84 (s, 3H, CH<sub>3</sub>), 7.30 (s, H), 7.32 (s, H), 8.26 (s, H),

1  
2  
3 12.05 (s, N<sup>+</sup>-H). <sup>13</sup>C NMR (150 MHz): 34.2, 116.9, 121.9, 136.8. <sup>11</sup>B NMR (193 MHz): -  
4  
5  
6  
7 1.06 (s). <sup>19</sup>F NMR (565 MHz): - 150.99 (s, <sup>10</sup>BF<sub>4</sub>) and -151.04 (s, <sup>11</sup>BF<sub>4</sub>) in 1:4 intensity  
8  
9  
10 ratio, which corresponding to the natural abundance of <sup>10</sup>B and <sup>11</sup>B isotopes in ca. 20%  
11  
12  
13 and ca. 80%, respectively. The NMR spectra of [HMIM][PF<sub>6</sub>] in D<sub>2</sub>O: <sup>1</sup>H NMR (600  
14  
15  
16 MHz): 3.65 (s, 3H, CH<sub>3</sub>), 7.16 (s, 2H), 8.37 (s, H). <sup>13</sup>C NMR (150 MHz): 35.3, 119.3,  
17  
18  
19 122.8, 134.8. <sup>31</sup>P NMR (243 MHz): -145.3 (sep, J = 709.17 Hz) <sup>19</sup>F NMR (565 MHz): -  
20  
21  
22  
23  
24 72.85 (d, J = 709.14 Hz)  
25  
26  
27  
28

29 *NMR spectra* were recorded on Bruker AV600 spectrometer at ambient temperature.

30  
31  
32 Standards according to Bruker almanac <sup>[43]</sup> were used. Water content in the ILs was  
33  
34  
35 controlled by Fischer titration using a KAS-01 MD apparatus.  
36  
37  
38  
39

40 *Electrochemical etching.* The etching was carried out in a PTFE cell of the original  
41  
42  
43 design (see Fig. 1). It consisted of a PTFE rod fitted with a PTFE nut with a 4 mm hole  
44  
45  
46 that allowed the silicon wafer to be pressed against a stainless steel rod, which served  
47  
48  
49 as a current collector. A PTFE nut also allows us to limit the etching area, so it remains  
50  
51  
52 constant throughout all experiments. In parallel with the silicon wafer, a platinum grid  
53  
54  
55  
56  
57  
58  
59  
60

1  
2  
3 cathode was fixed above the PTFE cell. The etching agent was placed on the surface of  
4  
5  
6  
7 the silicon wafer using a micropipette. The etching process was carried out in  
8  
9  
10 galvanostatic mode at current density in the range from 8 mA/cm<sup>2</sup> to 24 mA/cm<sup>2</sup> using a  
11  
12  
13 PC-piloted digital potentiostat IPC-Pro-MF (Econix). Etching time was varied from 30  
14  
15  
16  
17 minutes to 6 hours. After that, the silicon wafer was washed with ethyl alcohol and  
18  
19  
20  
21 stored in a high-purity argon atmosphere in a septum-sealed vial.  
22  
23

24  
25 *SEM/EDS*. Morphology of pristine and etched silicon surface was studied using a  
26  
27  
28 Hitachi SU8000 field-emission scanning electron microscope (FE-SEM). The images  
29  
30  
31  
32 were acquired in secondary electron mode at 20 kV accelerating voltage and the  
33  
34  
35  
36 working distance 8-10 mm. Energy-dispersive X-ray spectroscopy (EDS) was carried  
37  
38  
39  
40 out using an Oxford Instruments X-max 80 EDS system at 20 kV accelerating voltage  
41  
42  
43 and a working distance 15 mm. The samples were studied without metallization in order  
44  
45  
46 to avoid metal coating effects.<sup>[44]</sup>  
47  
48  
49  
50  
51  
52  
53  
54  
55  
56  
57  
58  
59  
60

1  
2  
3  
4 *Raman spectroscopy.* Raman spectra were acquired with a BWS415 spectrometer  
5  
6  
7 (BWTEK, Germany) with 785 nm laser, and with EnSpectr532 spectrometer (Enspectr,  
8  
9  
10 Russia), integrated with 532 nm laser and CX41 microscope (Olympus, Japan).  
11  
12

13  
14  
15 *Confocal microscopy.* Confocal microscopy was performed with Nikon A1 confocal  
16  
17  
18 microscope equipped with 401 nm and 514 nm lasers and spectral detector (Nikon,  
19  
20  
21  
22 Japan).  
23  
24  
25

## 26 **Summary**

27  
28  
29  
30  
31 High-purity porous silicon with uniform and size-controlled pores was produced using  
32  
33  
34 wet 1-methylimidazolium tetrafluoroborate as the etching solution. Such a non-volatile,  
35  
36  
37 non-flammable, and chemically and electrochemically stable system is a good  
38  
39  
40  
41 alternative to commonly used aggressive, toxic and dangerous HF.<sup>[45]</sup>1-  
42  
43

44  
45 Methylimidazolium tetrafluoroborate is easily synthesized and does not require special  
46  
47  
48 storage conditions. Moreover, it can be considered as a potentially recyclable etching  
49  
50  
51 agent. Besides, the etching process is very simple, secure and efficient with no need of  
52  
53  
54  
55 additional heating, control of potential or any other special precautions. All this makes  
56  
57  
58  
59  
60

1  
2  
3 the proposed technique suitable for scaling-up. Application of HF-free solvent-in-salt  
4  
5  
6  
7 system for eco-friendly etching is a novel approach with excellent practical  
8  
9  
10 opportunities.  
11  
12  
13  
14  
15  
16  
17  
18

### 19 **Conflicts of interest**

20  
21  
22  
23  
24 There are no conflicts to declare.  
25  
26  
27

### 28 **ASSOCIATED CONTENT**

#### 29 30 31 **Supporting Information.**

32  
33  
34  
35  
36  
37 Additional SEM data, NMR and Raman spectra are provided in the Supporting  
38  
39  
40  
41 Information.  
42  
43

44 This file is available free of charge.  
45  
46  
47

### 48 49 **AUTHOR INFORMATION**

#### 50 51 52 53 **Corresponding Author** 54 55 56 57 58 59 60

1  
2  
3 \* Dr. M. A. Syroeshkin  
4  
5  
6  
7

8 E-mail: syroeshkin@ioc.ac.ru  
9  
10  
11

12 \* Prof. Dr. V. V. Jouikov  
13  
14  
15

16  
17 E-mail: vjouikov@univ-rennes1.fr  
18  
19  
20

## 21 **Author Contributions**

22  
23  
24

25 All authors contributed equally.  
26  
27  
28

## 29 **Funding Sources**

30  
31  
32

## 33 **ACKNOWLEDGMENT**

34  
35  
36

37 (E.A.S., M.P.E., M.A.S. acknowledge the support by Russian Science Foundation Grant  
38  
39

40 17-73-20281. Electron microscopy and NMR spectra characterization were performed  
41  
42

43 at the Department of Structural Studies of Zelinsky Institute of Organic Chemistry,  
44  
45

46  
47 Moscow. Raman spectroscopy and confocal microscopy were performed by A.A.N. and  
48  
49

50 M.V.G., and were funded by the Ministry of Science and Higher Education of the  
51  
52

53  
54 Russian Federation within the State Assignment (project 0768-2020-0007).  
55  
56  
57  
58  
59  
60

1  
2  
3  
4 ABBREVIATIONS

5  
6 [BMIM][BF<sub>4</sub>], 1-Butyl-3-methylimidazolium tetrafluoroborate; EDS, energy dispersive X-  
7  
8  
9 ray spectroscopy; EMIMF·2.3HF, 1-ethyl-3-methylimidazolium oligofluorohydrogenate;  
10  
11  
12 IL, ionic liquid; [HMIM][BF<sub>4</sub>], 1-Methylimidazolium tetrafluoroborate; [HMIM][PF<sub>6</sub>], 1-  
13  
14 Methylimidazolium hexafluorophosphate; NMR, nuclear magnetic-resonance; PTFE,  
15  
16  
17 polytetrafluorethylene; PSi, porous silicon; SEM, scanning electron microscope; w-IL,  
18  
19  
20  
21  
22  
23 wet ionic liquids.  
24  
25

26  
27  
28 REFERENCES

- 29  
30  
31 1. Shin, D. H.; Kim, J. M.; Jang, C. W.; Kim, J. H.; Kim, S.; Choi, S. H. Effect of  
32  
33  
34 Layer Number and Metal-Chloride Dopant on Multiple Layers of  
35  
36  
37 Graphene/Porous Si Solar Cells. *J. Appl. Phys.* **2018**, 123 (12), 123101.  
38  
39  
40  
41 <https://doi.org/10.1063/1.5013169>.  
42  
43  
44  
45  
46 2. Mohammed, M. S.; Shlaga, R. A. Reflectivity Effect of the PS on Solar Cell  
47  
48  
49 Efficiency. *In Journal of Physics: Conference Series*; **2018**.  
50  
51  
52  
53 <https://doi.org/10.1088/1742-6596/1032/1/012027>.  
54  
55  
56  
57  
58  
59  
60

- 1  
2  
3  
4 3. Praveenkumar, S.; Lingaraja, D.; Mahiz Mathi, P.; Dinesh Ram, G. An  
5  
6  
7 Experimental Study of Optoelectronic Properties of Porous Silicon for Solar Cell  
8  
9  
10 Application. *Optik (Stuttg)*. **2019**, 178, 216-223.  
11  
12  
13 <https://doi.org/10.1016/j.ijleo.2018.09.176>.  
14  
15  
16  
17  
18 4. Juzeliū Nas, E.; Fray, D. J. Silicon Electrochemistry in Molten Salts. *Chem. Rev.*  
19  
20  
21 **2020**, 120, 3, 1690-1709. <https://doi.org/10.1021/acs.chemrev.9b00428>.  
22  
23  
24  
25  
26 5. Korotcenkov G., Rusu E., How to Improve the Performance of Porous  
27  
28  
29 Silicon-Based Gas and Vapor Sensors? Approaches and Achievements. *Phys.*  
30  
31  
32  
33 *Status Solidi Appl. Mater. Sci.*, **2019**, 216, 1900348.  
34  
35  
36  
37 <https://doi.org/10.1002/pssa.201900348>.  
38  
39  
40  
41 6. Wang J., Jia Z., Metal Nanoparticles/Porous Silicon Microcavity Enhanced  
42  
43  
44  
45 Surface Plasmon Resonance Fluorescence for the Detection of DNA. *Sensors*,  
46  
47  
48 **2018**, 18, 661. <https://doi.org/10.3390/s18020661>.  
49  
50  
51  
52  
53  
54  
55  
56  
57  
58  
59  
60

- 1  
2  
3  
4 7. Terracciano, M.; Rea, I.; Borbone, N.; Moretta, R.; Oliviero, G.; Piccialli, G.; De  
5  
6  
7 Stefano, L. Porous Silicon-Based Aptasensors: The Next Generation of Label-  
8  
9  
10 Free Devices for Health Monitoring. *Molecules* **2019**, 24 (12), 2216.  
11  
12  
13  
14 <https://doi.org/10.3390/molecules24122216>.  
15  
16  
17  
18 8. Ge, D.; Shi, J.; Wei, J.; Zhang, L.; Zhang, Z. Optical Sensing Analysis of Bilayer  
19  
20  
21 Porous Silicon Nanostructure. *J. Phys. Chem. Solids* **2019**, 130, 217–221.  
22  
23  
24  
25 <https://doi.org/10.1016/j.jpcs.2019.03.002>.  
26  
27  
28  
29 9. Harraz, F. A. Porous Silicon Chemical Sensors and Biosensors: A Review.  
30  
31  
32  
33 *Sensors Actuators, B Chem.* **2014**, 202, 897-912.  
34  
35  
36  
37 <https://doi.org/10.1016/j.snb.2014.06.048>.  
38  
39  
40  
41 10. Gopal, S.; Chiappini, C.; Penders, J.; Leonardo, V.; Seong, H.; Rothery, S.;  
42  
43  
44 Korchev, Y.; Shevchuk, A.; Stevens, M. M. Porous Silicon Nanoneedles  
45  
46  
47 Modulate Endocytosis to Deliver Biological Payloads. *Adv. Mater.* **2019**, 31  
48  
49  
50  
51 (12), 1806788. <https://doi.org/10.1002/adma.201806788>.  
52  
53  
54  
55  
56  
57  
58  
59  
60

- 1  
2  
3  
4 11. Park, Y.; Yoo, J.; Kang, M. H.; Kwon, W.; Joo, J. Photoluminescent and  
5  
6  
7 Biodegradable Porous Silicon Nanoparticles for Biomedical Imaging. *J. Mater.*  
8  
9  
10 *Chem. B.* **2019**, *7*, 6271-6292. <https://doi.org/10.1039/c9tb01042d>.  
11  
12  
13  
14  
15 12. Santos, H. A.; Mäkilä, E.; Airaksinen, A. J.; Bimbo, L. M.; Hirvonen, J. Porous  
16  
17  
18 Silicon Nanoparticles for Nanomedicine: Preparation and Biomedical  
19  
20  
21  
22 Applications. *Nanomedicine.* **2014**, *9*, 535–554.  
23  
24  
25 <https://doi.org/10.2217/nnm.13.223>.  
26  
27  
28  
29  
30 13. Tieu, T.; Alba, M.; Elnathan, R.; Cifuentes-Rius, A.; Voelcker, N. H. Advances in  
31  
32  
33 Porous Silicon-Based Nanomaterials for Diagnostic and Therapeutic  
34  
35  
36  
37 Applications. *Adv. Ther.* **2019**, *2* (1), 1800095.  
38  
39  
40 <https://doi.org/10.1002/adtp.201800095>.  
41  
42  
43  
44  
45 14. Zhang, D. X.; Esser, L.; Vasani, R. B.; Thissen, H.; Voelcker, N. H. Porous  
46  
47  
48 Silicon Nanomaterials: Recent Advances in Surface Engineering for Controlled  
49  
50  
51  
52 Drug-Delivery Applications. *Nanomedicine.* **2019**, *14*, 3213–3230.  
53  
54  
55 <https://doi.org/10.2217/nnm-2019-0167>.  
56  
57  
58  
59  
60

- 1  
2  
3  
4 15. Alhmoud, H., Brodoceanu, D., Elnathan, R., Kraus, T., Voelcker, N.H., A  
5  
6  
7 MACEing Silicon: Towards single-step etching of defined porous  
8  
9  
10 nanostructures for biomedicine, *Progress in Materials Science*. **2019**, 100636.  
11  
12  
13  
14 doi: <https://doi.org/10.1016/j.pmatsci.2019.100636>.  
15  
16  
17  
18 16. Jones, E. C. L.; Bimbo, L. M. Crystallisation Behaviour of Pharmaceutical  
19  
20  
21 Compounds Confined within Mesoporous Silicon. *Pharmaceutics* **2020**, 12 (3),  
22  
23  
24 214. <https://doi.org/10.3390/pharmaceutics12030214>.  
25  
26  
27  
28  
29 17. E. Quiroga-González, H. Föll, In: Porous Silicon: From Formation to Application,  
30  
31  
32 Ed. G. Korotchenkov, Ch.2, CRC Press, 2016, 29-46.  
33  
34  
35  
36  
37 18. Peng, J.; Liu, R.; Peng, L.; Jia, H. Calcium Gluconate Alleviates the Toxic Effect  
38  
39  
40 of Hydrofluoric Acid on Human Dermal Fibroblasts through the Wnt/B-catenin  
41  
42  
43  
44 Pathway. *Oncol. Lett.* **2018**, 16 (3), 2921–2928.  
45  
46  
47  
48 <https://doi.org/10.3892/ol.2018.8975>.  
49  
50  
51  
52  
53  
54  
55  
56  
57  
58  
59  
60

- 1  
2  
3  
4 19. V. Jouikov, A. Zizumbo, Eur. Pat. 16305617.9, 27.05.2016.  
5  
6  
7 <https://patentscope.wipo.int/search/en/detail.jsf?docId=WO2017203063>,  
8  
9  
10 accessed 10.06.2020.  
11  
12  
13  
14  
15 20. Zhao, S.; Zhang, Q.; Lv, Y.; Wang, X. An HF-Free Etching of SiO<sub>2</sub> for Soft  
16  
17  
18 Lithography. *IEEE Trans. Nanotechnol.* **2016**, 15 (4), 666–670.  
19  
20  
21 <https://doi.org/10.1109/TNANO.2016.2572120>.  
22  
23  
24  
25  
26 21. Kumar, V.; Potdevin, A.; Boutinaud, P.; Boyer, D. HF-Free Synthesis of K<sub>2</sub>SiF<sub>6</sub>  
27  
28  
29 and BaSiF<sub>6</sub> Nanoparticles by Thermal Decomposition. *Mater. Lett.* **2020**, 261,  
30  
31  
32 127123. <https://doi.org/10.1016/j.matlet.2019.127123>.  
33  
34  
35  
36  
37  
38 22. Teo, W. L.; Ariff, S. K. B.; Zhou, W.; Jana, D.; Phua, S. Z. F.; Zhao, Y. Solvent-  
39  
40  
41 and HF-Free Synthesis of Flexible Chromium-Based MIL-53 and MIL-88B.  
42  
43  
44 *ChemNanoMat* **2020**, 6 (2), 204–207. <https://doi.org/10.1002/cnma.201900665>.  
45  
46  
47  
48  
49  
50  
51  
52  
53  
54  
55  
56  
57  
58  
59  
60

- 1  
2  
3  
4 23. Fialho, L.; Almeida Alves, C. F.; Marques, L. S.; Carvalho, S. Development of  
5  
6  
7 Stacked Porous Tantalum Oxide Layers by Anodization. *Appl. Surf. Sci.* **2020**,  
8  
9  
10 511, 145542. <https://doi.org/10.1016/j.apsusc.2020.145542>.  
11  
12  
13  
14  
15 24. Greaves T. L., Drummond C. J., Protic ionic liquids: properties and applications.  
16  
17  
18 *Chem. Rev.* **2008**, 108, 206-237. <https://doi.org/10.1021/cr068040u>.  
19  
20  
21  
22  
23 25. Buzzeo M.C., Evans R.G., and Compton R.G., Non-haloaluminate room-  
24  
25  
26 temperature ionic liquids in electrochemistry—a review. *ChemPhysChem*, **2004**,  
27  
28  
29 5, 1106-1120. <https://doi.org/10.1002/cphc.200301017>.  
30  
31  
32  
33  
34 26. Silvester D.S., Compton R.G., Electrochemistry in Room Temperature Ionic  
35  
36  
37 Liquids: A Review and Some Possible Applications. *Zeitschrift Für*  
38  
39  
40 *Physikalische Chemie*, **2006**, 220(10), 1247–1274.  
41  
42 <https://doi.org/10.1524/zpch.2006.220.10.1247>.  
43  
44  
45  
46  
47  
48  
49 27. Liu H., Liu Y., Li J., Ionic liquids in surface electrochemistry. *Phys. Chem. Chem.*  
50  
51  
52 *Phys.*, **2010**, 12, 1685-1697. <https://doi.org/10.1039/B921469K>  
53  
54  
55  
56  
57  
58  
59  
60

- 1  
2  
3  
4 28. Cvjetko Bubalo, M.; Vidović, S.; Radojčić Redovniković, I.; Jokić, S. Green  
5  
6  
7 Solvents for Green Technologies. *J. Chem. Technol. Biotechnol.* **2015**, *90* (9),  
8  
9  
10 1631–1639. <https://doi.org/10.1002/jctb.4668>.  
11  
12  
13  
14  
15 29. Yoo, C. G.; Pu, Y.; Ragauskas, A. J. Ionic Liquids: Promising Green Solvents for  
16  
17  
18 Lignocellulosic Biomass Utilization. *Curr. Opin. Green Sustain. Chem.*, **2017**, *5*,  
19  
20  
21 5–11. <https://doi.org/10.1016/j.cogsc.2017.03.003>.  
22  
23  
24  
25  
26 30. Earle, M. J.; Seddon, K. R. Ionic Liquids. Green Solvents for the Future. *Pure*  
27  
28  
29 *and Applied Chemistry*, **2000**, *72*, 1391.  
30  
31  
32  
33 <https://doi.org/10.1351/pac200072071391>.  
34  
35  
36  
37  
38 31. Egorova, K. S.; Gordeev, E. G.; Ananikov, V. P. Biological Activity of Ionic  
39  
40  
41 Liquids and Their Application in Pharmaceuticals and Medicine. *Chem. Rev.*,  
42  
43  
44 **2017**, *117*, 7132–7189. <https://doi.org/10.1021/acs.chemrev.6b00562>.  
45  
46  
47  
48  
49  
50  
51  
52  
53  
54  
55  
56  
57  
58  
59  
60

- 1  
2  
3  
4 32. Janus E., Goc-Maciejewska I., Łozyn´ski M., Pernakb J., Diels–Alder reaction in  
5  
6  
7 protic ionic liquids. *Tetrahedron Lett.* **2006**, 47, 4079-4083.  
8  
9  
10 <https://doi.org/10.1016/j.tetlet.2006.03.172>.  
11  
12  
13  
14  
15 33. Azov, V. A.; Egorova, K. S.; Seitkalieva, M. M.; Kashin, A. S.; Ananikov, V. P.  
16  
17  
18 “Solvent-in-Salt” Systems for Design of New Materials in Chemistry, Biology  
19  
20  
21 and Energy Research. *Chem. Soc. Rev.*, **2018**, 47, 1250–1284.  
22  
23  
24 <https://doi.org/10.1039/c7cs00547d>.  
25  
26  
27  
28  
29  
30 34. Ramizy A., Ibrahim I. M., Hammadi M. A., The Effect of Etching Current Density  
31  
32  
33 on Porous Silicon Fabricated by Electrochemical Etching Process. *International*  
34  
35  
36 *Journal of Scientific & Engineering Research*, **2016**, 7 (4) 717-722.  
37  
38  
39  
40  
41 35. Al-Husseini A. M., Influence of Current Density on Morphology of  
42  
43  
44 Electrochemically Formed Porous Silicon. *Jordan J Phys*, **2016**, 9, 47.  
45  
46  
47  
48  
49  
50  
51  
52  
53  
54  
55  
56  
57  
58  
59  
60

- 1  
2  
3  
4 36. Susan M. A. B. H., Noda A., Mitsushima S., Watanabe M., Brønsted acid–base  
5  
6  
7 ionic liquids and their use as new materials for anhydrous proton conductors.  
8  
9  
10 *Chem. Comm.* **2003**, 938-939. <https://doi.org/10.1039/B300959A>  
11  
12  
13  
14  
15 37. Datasheets, SOLVIONIC SASite SME, [www.solvionic.com](http://www.solvionic.com), accessed  
16  
17  
18 10.06.2020.  
19  
20  
21  
22  
23 38. Stoppa A., Hunger J., Buchner R., Conductivities of Binary Mixtures of Ionic  
24  
25  
26 Liquids with Polar Solvents. *J. Chem. Eng. Data* **2009**, 54, 2, 472-479.  
27  
28  
29 <https://doi.org/10.1021/je800468h>  
30  
31  
32  
33  
34 39. Nakamura K., Shikata T., Systematic Dielectric and NMR Study of the Ionic  
35  
36  
37 Liquid 1-Alkyl-3-Methyl Imidazolium. *ChemPhysChem*, **2010**, 11(1), 285-294.  
38  
39  
40 <https://doi.org/10.1002/cphc.200900642>  
41  
42  
43  
44  
45  
46 40. Gu, L.; Hall, D. J.; Qin, Z.; Anglin, E.; Joo, J.; Mooney, D. J.; Howell, S. B.; Sailor,  
47  
48  
49 M. J. In Vivo Time-Gated Fluorescence Imaging with Biodegradable  
50  
51  
52  
53  
54  
55  
56  
57  
58  
59  
60

1  
2  
3 Luminescent Porous Silicon Nanoparticles. *Nat. Commun.* **2013**, 4 (1), 1–7.

4  
5  
6  
7 <https://doi.org/10.1038/ncomms3326>.

8  
9  
10  
11 41. Liu, C.; Jia, Z.; Lv, X.; Lv, C.; Shi, F. Enhancement of QDs' Fluorescence Based  
12 on Porous Silicon Bragg Mirror. *Phys. B Condens. Matter* **2015**, 457, 263–268.

13  
14  
15  
16  
17  
18 <https://doi.org/10.1016/j.physb.2014.10.005>.

19  
20  
21  
22 42. It should be noted that the technique for producing IL involves addition of acid to  
23  
24  
25  
26  
27 1-methylimidazole, and in order to exclude the presence of acid in the product  
28  
29  
30 the latter is taken in a minimal excess. The impurity of 1-methylimidazole in the  
31  
32  
33  
34 product is removed by repeated extraction with ethyl acetate. The resulting  
35  
36  
37 product is pure [HMIM][BF<sub>4</sub>] that has a characteristic shift of the acidic proton in  
38  
39  
40 acetonitrile near 12 ppm, which is identical to the published data (see Ref. 32).

41  
42  
43  
44 Taking into account the liquid state of the salt, it is actually a non-buffered  
45  
46  
47 solution with acid-base equilibrium. During etching, 1-methylimidazole, partially  
48  
49  
50  
51 formed by dissociation of the salt, can be oxidized and an appearing impurity of  
52  
53  
54 HBF<sub>4</sub>, even in such a small amount not being detected in all spectral data (the  
55  
56  
57  
58  
59  
60

1  
2  
3 shifts of all other protons remain the same after etching,  $^{11}\text{B}$  and  $^{19}\text{F}$  spectra  
4  
5  
6  
7 are also identical), can cause a significant high field shift of the acidic proton. In  
8  
9  
10 support of this explanation, we have taken a cyclic voltammetry measurement  
11  
12  
13 of [HMIM][BF<sub>4</sub>] under the same conditions as were during etching but in the  
14  
15  
16 presence of 1-methylimidazole. It was revealed that its oxidation begins at  
17  
18  
19 rather low potentials, namely +0.8 V vs. Ag/AgCl (the wave does not have a  
20  
21  
22 pronounced maximum because of high viscosity of the system), which is  
23  
24  
25 significantly lower than the real etching potential (> 2 V vs. Ag/AgCl). Also  $^1\text{H}$   
26  
27  
28 NMR measurement of [HMIM][BF<sub>4</sub>] in acetonitrile showed that the presence of  
29  
30  
31  
32 3 mol% HBF<sub>4</sub> (a minimal amount that can be added to a NMR tube with  
33  
34  
35 reasonable accuracy) causes a high field shift of the acidic NH-proton signal by  
36  
37  
38  
39  
40  
41  
42 3 ppm.  
43  
44  
45

46 43. Bruker corporation, Almanac, 2010, ISBN 978-3-929431-24-7, *Chemical Shift*

47  
48  
49 *Ranges and Standards for Selected Nuclei*, <https://www.pascal->

50  
51  
52  
53 [man.com/pulseprogram/Almanac2010.pdf](https://www.pascal-man.com/pulseprogram/Almanac2010.pdf), accessed 10.06.2020  
54  
55  
56  
57  
58  
59  
60

- 1  
2  
3  
4 44. Kashin, A. S.; Ananikov, V. P. A SEM Study of Nanosized Metal Films and Metal  
5  
6  
7 Nanoparticles Obtained by Magnetron Sputtering. *Russ. Chem. Bull.* **2011**, 60  
8  
9  
10 (12), 2602–2607. <https://doi.org/10.1007/s11172-011-0399-x>.  
11  
12  
13  
14  
15 45. It should be noted that a technique of etching silicon using ionic liquid 1-ethyl-3-  
16  
17  
18 methylimidazolium oligofluorohydrogenate (EMIMF·2.3HF) has been published  
19  
20  
21 in the literature. However, HF is also actually present in such a system. Raz,  
22  
23  
24 O., Starosvetsky, D., Tsuda, T., Nohira, T., Hagiwara, R., Ein-Eli, Y.  
25  
26  
27  
28  
29 Macroporous Silicon Formation on n-Si in Room-Temperature  
30  
31  
32 Fluorohydrogenate Ionic Liquid, *Electrochem. Solid-State Lett.*, **2007**, 10, D25-  
33  
34  
35  
36 D28. <https://doi.org/10.1149/1.2409058>.  
37  
38  
39  
40  
41  
42  
43  
44  
45  
46  
47  
48  
49  
50  
51  
52  
53  
54  
55  
56  
57  
58  
59  
60

1  
2  
3  
4  
5  
6  
7  
8  
9  
10  
11  
12  
13  
14  
15  
16  
17  
18  
19  
20  
21  
22  
23  
24  
25  
26  
27  
28  
29  
30  
31  
32  
33  
34  
35  
36  
37  
38  
39  
40  
41  
42  
43  
44  
45  
46  
47  
48  
49  
50  
51  
52  
53  
54  
55  
56  
57  
58  
59  
60

[For Table of Contents](#)

